AIAA JOURNAL
Vol. 30, No. 10, October 1992

Mobilities of Periodic Structures in Terms of Asymptotic Modal Properties

T. Igusa* and Y. Tang†
Northwestern University, Evanston, Illinois 60208

The natural frequencies of periodic structures lie in distinct frequency bands and become densely spaced when the number of periodic segments is large. This paper shows that within such frequency bands the structure has modal properties with asymptotic characteristics. This feature of periodic structures is used to develop an asymptotic integral expression for the mobility function. The asymptotic theory provides an alternate view of periodic structures that complements existing wave and transfer matrix based methods.

Nomenclature

$A(\omega)$, $B(\omega)$	= functions related to modal mass
C	= constant related to modal mass
c	= wave speed in rod
d_k	= displacement at junction k
EA	= axial stiffness of rod
e_m	= relative error
f_k	= force at junction k
$H(\omega,\eta,\omega_f)$	= modal frequency response function
i	$=\sqrt{(-1)}$
j	= mode number
k_f	= junction number of applied force
k_r	= junction number of response
l	= length of period segment
M_j	= jth modal mass
$M(\omega)$	= modal mass function
m_0	= lumped mass
N	= total number of periodic segments
$q(x_r,x_f,\omega_f)$	= function for asymptotic mobility
T	= transfer matrix
$t_{ij}(\omega)$	= (i,j)th element of transfer matrix
$w(x,\omega)$	= displacement function for a periodic segment
x	= spatial coordinate
x_f	= location of applied force
x_r	= location of response
$Y(x_r,x_f,\omega_f)$	= mobility function
$\beta(\omega)$	= frequency spacing function
β_j	= jth normalized frequency spacing
$\Delta\omega_j$	= jth natural frequency increment
$\delta(\cdot)$	= Dirac delta function
η_j	= jth modal loss factor
$\eta(\omega)$	= loss factor function
μ	= logarithm of eigenvalue of transfer matrix
$\rho(x)$	= mass density
$\phi(x,\omega_f)$	= mode shape function
$\phi_j(x)$	= jth mode shape
Ω	= spatial domain of the structure
ω	= natural frequency
ω_f	= excitation frequency
ω_j	= jth natural frequency
$\omega_L(n)$	= lower bound of the nth passband
$\omega_U(n)$	= upper bound of the nth passband

Received March 2, 1991; revision received Dec. 24, 1991; accepted for publication Dec. 31, 1991.

*Associate Professor, Civil Engineering. Member AIAA.
†Research Assistant, Civil Engineering.

Introduction

A PERIODIC structure consists of a sequence of spatially repeated segments. The behavior of such structures under dynamic loads has been examined using wave analysis[1,2] and transfer matrices.[3] Recently, several new methods have been developed using wave reflection and transmission matrices,[4] phase closure,[5] alternative wave propagation analysis,[6] and receptance theory.[7]

One important characteristic of periodic structures is that, as the number of repeated segments N increases, the natural frequencies become densely grouped within distinct transmission passbands. This suggests examining the asymptotic properties of the structure in the limit of large N.

Crandall[8,9] and Dowell and Kubota[10] proved that a wide variety of structures have modal properties with well-behaved asymptotic limits and demonstrated that this property provides valuable insight into dynamic analysis. They examined spatial averages of responses to wideband and harmonic loads and showed that the exact results converge to their asymptotic expressions for increasing modal densities.

The present paper shows that symmetric, monocoupled periodic structures are also characterized by well-behaved asymptotic modal properties. These properties are used to evaluate the response of periodic structures to harmonic loads. As the number of periodic segments increases, it is shown that the harmonic response functions asymptotically approach an integral form similar to that developed by Skudrzyk[11,12] for more fundamental, nonperiodic structures.

The analysis reveals two asymptotic parameters: the damping loss factor η and the product $N\eta$. Xu[13] investigated the relationship between the parameter $N\eta$ and the accuracy of an asymptotic response expression in an entirely different context. It is found herein that his results also apply to periodic structures. For sufficiently large $N\eta$, the asymptotic limit of small η yields further simplifications in the harmonic response expressions that are similar to results obtained by Skudrzyk[11,12] for nonperiodic structures.

The paper begins with an asymptotic harmonic response expression for arbitrary structures, which is a generalization of Skudrzyk's results. Next, after reviewing the expressions for the mode shapes and natural frequencies of symmetric, monocoupled periodic structures, new expressions for the modal masses are derived. Then it is shown how these expressions can be developed into asymptotic forms. Finally, the results are combined to develop an asymptotic integral expression for harmonic response. The asymptotic theory is illustrated by a continuous rod with regularly spaced lumped masses.

Asymptotic Mobility Analysis

Consider a continuous (not necessarily periodic) linear structure subjected to a harmonic force $\exp(-i\omega_f t)$ at a point x_f. The mobility $Y(x_r,x_f,\omega_f)$ is defined as the response velocity at a point x_r divided by the forcing term $\exp(-i\omega_f t)$. One method of obtaining the mobility function is by using modal (normal mode) coordinates.

Let the natural frequencies, modal loss factors, and mode shapes be denoted by ω_j, η_j, and $\phi_j(x)$, respectively. Define modal masses

$$M_j \equiv \int_\Omega \rho(x)\ \phi_j^2\ (x)\ \mathrm{d}x \tag{1}$$

where $\rho(x)$ is the mass density. Also let

$$H(\omega,\eta,\omega_f) \equiv (\omega^2 - i\eta\omega\omega_f - \omega_f^2)^{-1} \tag{2}$$

be the frequency response function for an oscillator with natural frequency ω and loss factor η. Then, it is well known that the modal expansion for the mobility function is[14]

$$Y(x_r,x_f,\omega_f) = -i\omega_f \sum_{j=1}^{\infty} \phi_j(x_r)\phi_j(x_f)H(\omega_j,\eta_j,\omega_f)\ M_j^{-1} \tag{3}$$

Skudrzyk[11,12] found that the mobility function for many fundamental vibrating systems, including rods, beams, plates, and cylindrical shells, can be approximated by an integral form at sufficiently high frequencies. The basic assumption is that the mode density is sufficiently great, and the loss factors are sufficiently high so that individual resonance peaks cannot be observed. The derivation of this integral form is briefly reviewed to establish notation.

The spacing of natural frequencies is measured by a dimensionless modal parameter

$$\beta_j \equiv \frac{\omega_{j+1}-\omega_j}{\omega_j} = \frac{\Delta\omega_j}{\omega_j} \tag{4}$$

where $\Delta\omega_j \equiv \omega_{j+1}-\omega_j$. It is assumed that the modal quantities β_j, η_j, $\phi_j(x_r)$, $\phi_j(x_f)$, and M_j vary smoothly with mode number j so that they can be naturally extended to continuous functions of frequency ω. These continuous functions, which are denoted by $\beta(\omega)$, $\eta(\omega)$, $\phi(x,\omega)$, and $M(\omega)$, must be consistent with the corresponding modal quantities, i.e., at the natural frequencies $\omega=\omega_j$, the functions must satisfy

$$\beta(\omega_j) = \beta_j \tag{5}$$

$$\eta(\omega_j) = \eta_j \tag{6}$$

$$\phi(x_r,\omega_j) = \phi_j(x_r), \qquad \phi(x_f,\omega_j) = \phi_j(x_f) \tag{7}$$

$$M(\omega_j) = M_j \tag{8}$$

Next a function is defined in terms of these modal functions,

$$q(x_r,x_f,\omega) \equiv \frac{\phi(x_r,\omega)\phi(x_f,\omega)}{M(\omega)\beta(\omega)\omega} \tag{9}$$

Then the mobility expansion in Eq. (3) is expressed in terms of the q function

$$Y(x_r,x_f,\omega_f) = -i\omega_f \sum_{j=1}^{\infty} q(x_r,x_f,\omega_j)\ H(\omega_j,\eta_j\ \omega_f)\ \Delta\omega_j \tag{10}$$

The final step is to consider the limiting case of closely spaced natural frequencies: the sum in Eq. (10) converges to the Riemann integral

$$Y(x_r,x_f,\omega_f) = -i\omega_f \int_0^{\infty} q(x_r,x_f,\omega)\ H[\omega,\eta(\omega),\omega_f]\ \mathrm{d}\omega \tag{11}$$

Skudrzyk[11,12] developed specific forms for the functions in Eqs. (5), (7), and (8) for the aforementioned fundamental vibrating systems. Herein, the integral form for the mobility is used to study monocoupled periodic systems.

Modal Properties of Symmetric, Monocoupled Periodic Systems

Figure 1 shows a schematic of a periodic structure. The numbered blocks represent repeating segments, and d_k and f_k are the displacements and forces at the kth junction. The structure is monocoupled if d_k and f_k are scalars. In the first part of this section, the expressions for the natural frequencies and mode shapes of monocoupled periodic structures are reviewed. Then new expressions for the model masses are derived; these are needed in the mobility expressions of the preceding section.

The transfer matrix approach[1-3] is used to develop the basic equations for the periodic structure. If the structure is vibrating at a frequency ω, the 2×2 transfer matrix $\boldsymbol{T}$ relates the displacements and forces of two successive junctions:

$$\begin{bmatrix} d_{k+1} \\ f_{k+1} \end{bmatrix} = \boldsymbol{T} \begin{bmatrix} d_k \\ f_k \end{bmatrix} \tag{12}$$

The elements of the transfer matrix,

$$\boldsymbol{T} = \begin{bmatrix} t_{11}(\omega) & t_{12}(\omega) \\ t_{21}(\omega) & t_{22}(\omega) \end{bmatrix} \tag{13}$$

are functions of ω determined by the segment's dynamic properties. The periodic property of the structure gives the relationship between the displacements and forces at the ends of the structure:

$$\begin{bmatrix} d_N \\ f_N \end{bmatrix} = \boldsymbol{T}^N \begin{bmatrix} d_0 \\ f_0 \end{bmatrix} \tag{14}$$

This relationship is needed to determine the structure's modal properties.

If each segment is symmetric, then $t_{11}(\omega)=t_{22}(\omega)$, and the Nth power of the transfer matrix becomes[15]

$$\boldsymbol{T}^N = \begin{bmatrix} \cosh(N\mu) & \dfrac{\sinh(N\mu)}{\sinh(\mu)}\ t_{12}(\omega) \\ \dfrac{\sinh(N\mu)}{\sinh(N\mu)}\ t_{21}(\omega) & \cosh(N\mu) \end{bmatrix} \tag{15}$$

where

$$\mu \equiv -i\cos^{-1}[t_{11}(\omega)] \tag{16}$$

The properties of the transfer matrix and the parameter μ have been studied in depth by Mead[2] and Keane and Price.[7]

The modal properties of the period structure with free ends are obtained by substituting $f_0=f_N=0$ into Eq. (14). It follows[15] that the natural frequencies are given by the solution of

$$\mathrm{Im}\mu = \cos^{-1}[t_{11}(\omega_j)] = \frac{j\pi}{N} \tag{17}$$

For continuous periodic structures, there are an infinite number of solutions of Eq. (17) for each j, where each solution corresponds to a different passband. The lower and upper limiting frequencies of the nth passband, which are denoted $\omega_L(n)$ and $\omega_U(n)$, are defined by the following conditions:

$$\omega_U(n-1) < \omega_L(n) < \omega_U(n) \tag{18}$$

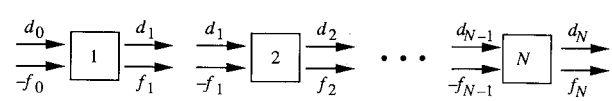

Fig. 1 Forces and displacements in a periodic structure.

$$|t_{11}(\omega)| \leq 1 \text{ for } \omega_L(n) \leq \omega \leq \omega_U(n) \tag{19}$$

$$|t_{11}(\omega)| > 1 \text{ for } \omega_U(n-1) \leq \omega \leq \omega_L(n) \tag{20}$$

The mode number j in Eq. (17) ranges over all nonnegative integers, where it is understood that ω_j for $j \leq N$ corresponds to the first passband, ω_j for $N < j \leq 2N$ corresponds to the second passband, and so on. The corresponding mode shapes[14] at the kth junction, for $k = 0, 1, \ldots, N$, are determined by Eq. (14),

$$\phi_j(x_k) = \cos \frac{jk\pi}{N} \tag{21}$$

The coordinate $x_k \equiv kl$ is the location of the kth junction measured from the left end of the structure.

The modal mass M_j is defined by Eq. (1) where the domain Ω represents all values of x from 0 to Nl. Equation (21) gives values for the mode shape only at the endpoints of the periodic segments; the problem is to determine $\phi_j(x)$ in the interior of each segment.

Consider the periodic segment at the left end of the structure. If the left end of this segment has a unit harmonic displacement $\exp(-i\omega t)$ and the right end is fixed, then, by dynamic analysis, it is possible to obtain the displacement $w(x,\omega)\exp(-i\omega t)$ along the entire segment. By superposition and the use of symmetry, the jth modal displacement along the interior of the segment is

$$\phi_j(x) = \phi_j(0)w(x,\omega) + \phi_j(l)w(l-x,\omega) \tag{22}$$

for $0 \leq x \leq l$. This argument can be repeated to obtain the mode shape along the interiors of all remaining periodic segments. Substituting the mode shape result into Eq. (1), using Eq. (21), and simplifying the series expansions yield expressions for the modal masses. The derivation details are shown in the Appendix; the final result is found to be relatively simple:

$$M_j = NC_j\left[A(\omega_j) + B(\omega_j)\cos\frac{j\pi}{N}\right] \tag{23}$$

where

$$A(\omega) \equiv \int_0^l \rho(x)w^2(x,\omega)\,dx \tag{24}$$

$$B(\omega) \equiv \int_0^l \rho(x)w(x,\omega)w(l-x,\omega)\,dx \tag{25}$$

$$C_j \equiv \begin{cases} 2 & j = 0, N, 2N, \ldots, \\ 1 & \text{all other } j \end{cases} \tag{26}$$

Mobilities of Symmetric, Monocoupled Periodic Structures

The results of the preceding two sections are combined to derive asymptotic integral expressions for the mobility of symmetric, monocoupled periodic structures. The first step is to obtain expressions for the frequency-dependent functions $\beta(\omega)$, $\phi(x,\omega)$, and $M(\omega)$.

The frequency space parameter β_j is obtained using Eqs. (4) and (17):

$$\beta_j \equiv \frac{\omega_{j+1}-\omega_j}{\omega_j} = \frac{\mathrm{Im}\mu_{j+1}-\mathrm{Im}\mu_j}{\omega_j}\left(\frac{\mathrm{Im}\mu_{j+1}-\mathrm{Im}\mu_j}{\omega_{j+1}-\omega_j}\right)^{-1} \approx \frac{\pi}{N\omega_j}\left(\frac{\partial \mathrm{Im}\mu_j}{\partial\omega_j}\right)^{-1} \tag{27}$$

where the derivative is used to approximate the difference in parenthesis. A natural definition of the function $\beta(\omega)$ is obtained by replacing ω_j by ω and using Eq. (17) for the derivative:

$$\beta(\omega) \equiv \frac{\pi}{N\omega}\left(\frac{\partial\{\cos^{-1}[t_{11}(\omega)]\}}{\partial\omega}\right)^{-1} \tag{28}$$

The mode shape function is obtained by combining Eqs. (17) and (21) to yield

$$\phi(x_k,\omega) \equiv \cos(k\,\mathrm{Im}\mu) = \cos\{k\cos^{-1}[t_{11}(\omega)]\} \tag{29}$$

Finally, the modal mass function is obtained by combining Eqs. (17) and (23)

$$M(\omega) \equiv N[A(\omega) + B(\omega)t_{11}(\omega)] \tag{30}$$

This is consistent with Eq. (23) for all values of ω_j except when $j = 0, N, 2N, \ldots$ [see Eq. (26)] that correspond to either the upper or lower frequency of each passband. This may result in small errors in the asymptotic results.

For an increasing number of periodic segments, the natural frequencies become proportionately dense in each passband, as indicated by the fact that $\beta(\omega)$ is inversely proportional to N. However, the mode shape, viewed as a function of natural frequency, is independent of N. In addition, the modal mass is proportional to N, as expected. The conclusions are that the modal properties of periodic structures do not have irregular or discontinuous behavior for increasing N, and that the functions in Eqs. (28–30) can be used as asymptotic forms of these properties.

The results in Eqs. (28–30) are combined to obtain an expression for the q function in Eq. (9). For an input force at junction k_f and output velocity at junction k_r, which corresponds to locations $x_f = lk_f$ and $x_r = lk_r$, the q function is

$$q(x_r,x_f,\omega) = \frac{\partial\{\cos^{-1}[t_{11}(\omega)]\}}{\partial\omega} \times \frac{2\cos\{k_r\cos^{-1}[t_{11}(\omega)]\}\cos\{k_f\cos^{-1}[t_{11}(\omega)]\}}{[A(\omega)+B(\omega)t_{11}(\omega)]\pi} \tag{31}$$

Substituting this into Eq. (11) yields the asymptotic integral form for the mobility.

The q function is independent of N. This is expected because the mobility integral in Eq. (11) is the asymptotic form for large N. The natural question is: What is the accuracy of this asymptotic form?

Xu[13] examined the accuracy of an asymptotic integral mobility expression that is similar to Eq. (11) but was developed for a discrete system of coupled oscillators. He derived an error estimate in terms of the natural frequency spacing β and the modal loss factor η. The maximum relative error, which was rigorously derived using series expansions and contour integrals, was found to be

$$e_m \approx \frac{2\sqrt{1+\pi^2}}{\pi}\exp\left(-\pi\frac{\eta}{\beta}\right) \tag{32}$$

It would be difficult to derive a similar error estimate for periodic structures. However, since the integral forms for the mobility are similar, it is believed that the expression in Eq. (32) applies herein. The final result, obtained by substituting the expression for β in Eq. (28) into Eq. (32), is

$$e_m \approx \frac{2\sqrt{1+\pi^2}}{\pi}\exp\left(-\omega\eta N\frac{\partial\{\cos^{-1}[t_{11}(\omega)]\}}{\partial\omega}\right) \tag{33}$$

This shows that the asymptotic parameter is not N but rather the product $N\eta$. The expression also shows that the error decreases exponentially as $N\eta$ increases; the example in the next section shows that the error can be quite small even if $N\eta$ is less than unity.

This section concludes with a second asymptotic analysis of the mobility for the case of small damping, i.e., $\eta \to 0$. It is assumed that the product $N\eta$ is always sufficiently large so that the first asymptotic result in Eqs. (11) and (31) remains valid. The q function is independent of η; the damping term appears only in the frequency response function $H(\omega,\eta,\omega_f)$ in Eq. (11). The real part of $H(\omega,\eta,\omega_f)$ remains a rational function, but it can be shown by standard limit analysis[16] that the imaginary part simplifies to

$$\mathrm{Im}H(\omega,\eta,\omega_f) \to \frac{\pi}{2\omega_f}\,\delta(\omega-\omega_f) \tag{34}$$

Substituting into Eq. (11) yields

$$\mathrm{Re}Y(x_r,x_f,\omega_f) \to \frac{\pi}{2}\,q(x_r,x_f,\omega) \tag{35}$$

This shows that the real part of the mobility has an asymptotic limit for small damping that is independent of damping. Skudrzyk[11,12] had a similar conclusion for certain nonperiodic structures. Equation (35) also gives a clear physical meaning to the q function: it is proportional to the real part of the mobility in the limit of small damping.

Example Application

The results derived herein are valid for any symmetric, monocoupled periodic structure. However, for purpose of illustration, it is useful to apply the theory to a simple example.

Consider a uniform rod of length Nl. Attached at equal intervals l are lumped masses of magnitude m_0 at the interior points and $m_0/2$ at the endpoints, as shown in Fig. 2. Thus, the periodic segments of the structure consist of a rod of length l with masses $m_0/2$ at the end points. It is convenient to define the wave speed in the rod without masses, $c=\sqrt{EA/\rho}$.

Expressions for the mobility are developed for arbitrary values of the structural parameters. However, in the figures numerical results are shown for the special case where $\rho l = m_0$ and $l/c = 1$ s.

The element $t_{11}(\omega)$ of the transfer matrix is given by

$$t_{11}(\omega) = \cos\frac{\omega l}{c} - \frac{m_0\omega}{2\rho c}\sin\frac{\omega l}{c} \tag{36}$$

Substituting this into Eq. (17) yields the frequency equation. The natural frequencies are plotted with respect to mode number in Fig. 3 for the case where the structure has the properties described earlier and $N=10$ segments. The figure also shows the locations of the passbands, as defined by Eqs. (18–20). Although the natural frequencies are widely spaced in the first passband, they become more densely spaced at the higher passbands. Furthermore, as the number of periodic segments N increases, the width of the passbands does not change; therefore, the natural frequencies become more closely spaced.

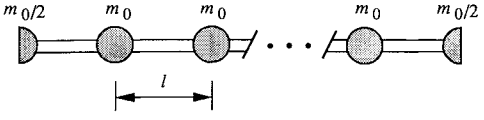

Fig. 2 Example periodic structure.

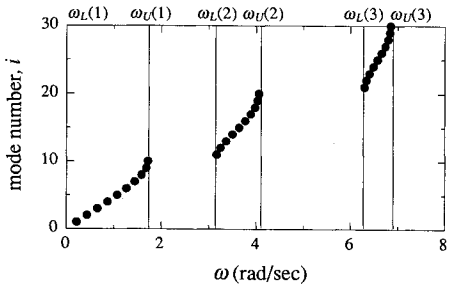

Fig. 3 Natural frequencies and passbands for $N=10$.

The behavior of the natural frequency spacing is illustrated by a plot of the parameter β in Fig. 4a. To keep the result independent of N, the product $N\beta$ is plotted with respect to natural frequency. At higher passbands the product $N\beta$ becomes smaller, indicating more densely spaced natural frequencies.

To obtain modal masses, the displacement function $w(x,\omega)$ is needed. For the rod with lumped masses, this is

$$w(x,\omega) = \frac{\sin[c^{-1}\omega(l-x)]}{\sin(c^{-1}\omega l)} \tag{37}$$

Substituting this expression into Eqs. (24) and (25) yields

$$A(\omega) = \frac{2\omega l - c\sin(2c^{-1}\omega l)}{4\omega\sin^2(c^{-1}\omega l)}\rho + \frac{m_0}{2} \tag{38}$$

$$B(\omega) = \frac{-\omega l\cos(c^{-1}\omega l) + c\sin(c^{-1}\omega l)}{2\omega\sin^2(c^{-1}\omega l)}\rho \tag{39}$$

The modal masses are determined by substituting these results into Eq. (30). Figure 4b plots the continuous form of the modal mass function in Eq. (30). To keep the result independent of N, the ratio $M(\omega)/N$ is plotted with respect to natural frequency. The modal masses are large at the lower end of the second and third passbands. This indicates that the motion of the continuous rod is large in the interior of the periodic segments and is small at the junctions, where the lumped masses are located.

Figure 4c plots the q function. Within each passband, $q(\omega)$ is small for low frequencies because of large modal masses and is large for high frequencies because of small frequency spacing.

Figures 5a and 5b show the real and imaginary parts of the driving-point mobility function, where the harmonic force and velocity response are both at the left end of the periodic structure and the loss factor is $\eta = 0.02$. Exact results, computed using standard transfer matrix analysis,[15] are plotted for

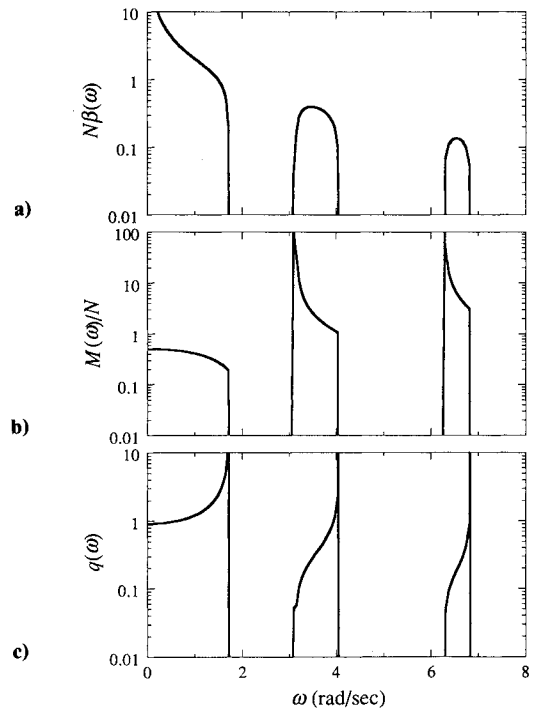

Fig. 4 Continuous modal functions: a) normalized frequency spacing, b) normalized modal mass and c) q function.

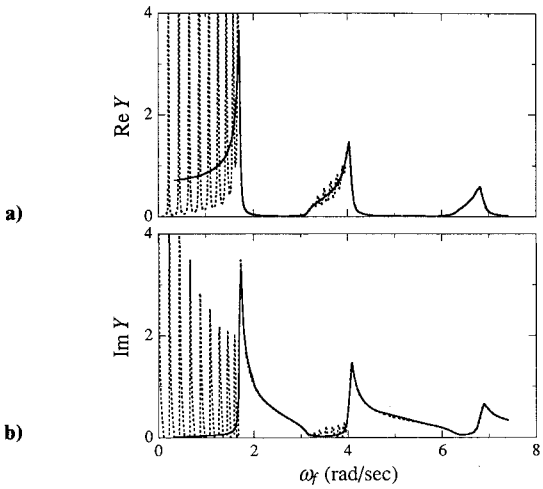

Fig. 5 Mobility function for $N = 10$ and $\eta = 0.02$: a) real part, b) imaginary part, - - - - - exact, and ——— asymptotic.

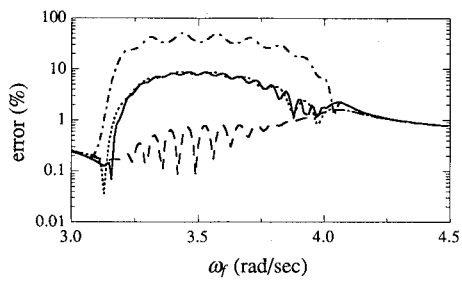

Fig. 6 Percent error of mobility function: - · - · - $N = 10$, $\eta = 0.02$; - - - - $N = 10$, $\eta = 0.04$; ——— $N = 20$, $\eta = 0.02$; - - - $N = 20$, $\eta = 0.04$.

$N = 10$ and are compared with the asymptotic mobility given in Eq. (11). The exact mobility has clearly defined resonance peaks in the first passband because the frequencies are widely spaced. Therefore, the asymptotic mobility is not expected to be accurate in this frequency range. (However, the asymptotic result follows the general trend of the fluctuating exact curve. This suggests that the mean-value method proposed by Skudrzyk[12] may be applicable to the analysis of the response at this passband.) At higher passbands, where the natural frequencies are more densely spaced, the asymptotic results match the exact curves more closely.

Figure 6 examines the relative errors of the asymptotic mobility for frequencies in the second passband. Four curves, obtained by comparing exact and asymptotic analyses for $\eta = 0.02$ and 0.04 and $N = 10$ and 20, are shown. The errors for $N = 10$ and $\eta = 0.04$ are nearly equal to those for $N = 20$ and $\eta = 0.02$. This agrees with Eqs. (32) and (33), which show that the error depends on the product $N\eta$.

To evaluate the accuracy of the error estimate, Eq. (33) is evaluated at $\omega = 3.5$ rad/s, which corresponds to the maximum value of the error in the second passband. The results are $e_m = 42.3\%$ for $N\eta = 0.2$, $e_m = 8.5\%$ for $N\eta = 0.4$, and $e_m = 0.35\%$ for $N\eta = 0.8$. The results are reasonable for the first two cases. However, in the last case the true error is larger than the estimate, which indicates that there is another source of error in the analysis. This additional error, which is around 1%, may have several possible origins: the slight inconsistency of the modal mass function noted after Eq. (30), the fact that the error estimate in Eqs. (32) and (33) was developed for a much simpler problem,[13] and the round-off error in the numerical computations.

To investigate the limit of small damping, a periodic structure with $N = 100$ and $\eta = 0.004$ is studied. The real part of the mobility is computed using exact equations and compared with the small-damping asymptotic result in Eq. (35). The results, which are plotted in Fig. 7, confirm that the real part of the mobility is proportional to the q function.

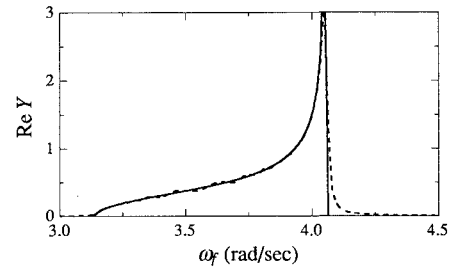

Fig. 7 Real part of the mobility function for $N = 100$ and $\eta = 0.004$: - - - - exact; ——— asymptotic.

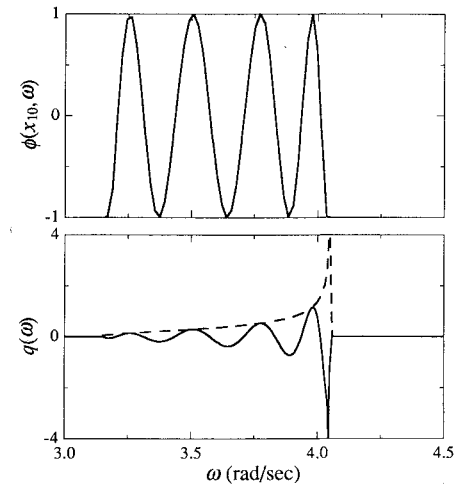

Fig. 8 Modal functions for cross mobility between 1st and 10th segments: a) mode shape function; b) q function, - - - driving-point mobility, ——— cross-mobility.

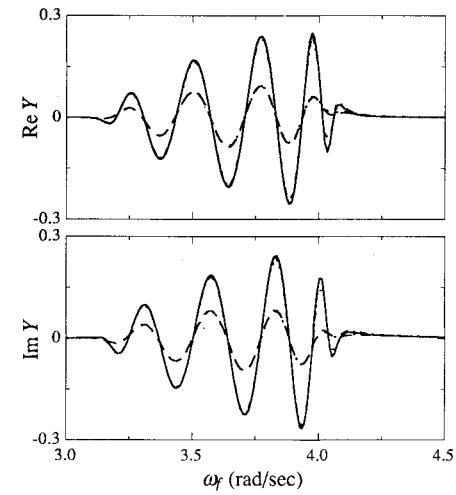

Fig. 9 Cross mobility between 1st and 10th segments: a) real part; b) imaginary part, - · - · - exact, $\eta = 0.02$; ——— asymptotic, $\eta = 0.02$; - - - - - - exact, $\eta = 0.04$; - - - - asymptotic, $\eta = 0.04$.

Figures 5–7 are for the driving-point mobility where the velocity response is determined at the same location as the point of application of the input force. To consider the cross mobility between different points, the mode shape function $\phi(x_k, \omega)$ in Eq. (29) must be evaluated and substituted into the q function in Eq. (31). For a force applied at the left end of the structure and the velocity response at the 10th junction, the mode shape function $\phi(x_{10}, \omega)$ and the corresponding q function are shown in Figs. 8a and 8b. For comparison, the q function for the driving-point mobility is also shown in Fig. 8b. As expected, $\phi(x_{10}, \omega)$ is oscillatory, which makes the q function also oscillatory. This leads to two predictions: the

mobility will be oscillatory with respect to the forcing frequency, and the magnitude of the mobility will decrease for increased damping. The second prediction will occur because oscillations of the q function in the integrand in Eq. (11) will cause cancellation effects. These cancellation effects are more pronounced when $H(\omega,\eta,\omega_f)$ becomes a smoother function of ω, that will occur as η increases.

These predictions are confirmed by plots of the real and imaginary parts of the cross mobility in Figs. 9a and 9b. The exact and asymptotic cross mobilities for $\eta = 0.02$ and 0.04 and $N = 40$ are shown in each figure. The asymptotic cross mobilities are virtually indistinguishable from the exact results. The plots also show that the cross mobilities are oscillatory with amplitudes that decrease as the damping increases from $\eta =$ 0.02 to 0.04.

Summary and Conclusions

Harmonic response expressions are developed for symmetric, monocoupled periodic structures using asymptotic techniques. The approach offers a different view of periodic structures that complements existing wave and transfer matrix-based methods. The following conclusions are made:

1) Periodic structures have modal properties with well-behaved asymptotic behavior. This permits the use of asymptotic modal techniques, originally set forth by Crandall[8,9] and Dowell and Kubota,[10] to the systematic study of such structures.

2) After the first passband, the modal expansions for the mobility function converge exponentially to an integral form with respect to the parameter $N\eta$. This integral form is a generalization of that developed by Skudrzyk[11,12] for more fundamental (nonperiodic) structures. The error estimate is found to be similar to one developed by Xu[13] for a simpler problem.

3) The asymptotic form of the mobility is related to a function defined over each passband in terms of asymptotic modal properties. This function is independent of the number of periodic segments and the modal loss factor.

4) In the limit of small damping, the real part of the mobility is directly proportional to the aforementioned function.

5) A modal interpretation is given for the behavior of cross mobilities between separate points of the periodic structure. This interpretation shows dependence on the distance between the points on the structure and on the modal loss factors and independence with respect to the total number of periodic segments.

Appendix

The modal mass is obtained by extending the mode shape expression in Eq. (22) to the entire periodic structure and substituting the result into Eq. (1). The result of the integration is

$$M = \sum_{k=1}^{N} \int_0^l \rho[x+(k-1)l] \times \{\phi_j[(k-1)l]w(x,\omega) + \phi_j(kl)w(l-x,\omega)^2\, dx = A(\omega)\sum_{k=1}^{N}\{\phi_j^2[(k-1)l] + \phi_j^2(kl)\} + 2B(\omega)\sum_{k=1}^{N}\phi_j[(k-1)l]\phi_j(kl) \quad \text{(A1)}$$

where $A(\omega)$ and $B(\omega)$ are given in Eqs. (24) and (25). This is simplified by making use of the following identities:

$$\sum_{k=1}^{N} \cos^2 \frac{kj\pi}{N} = \frac{N}{2} \quad \text{(A2)}$$

$$\sum_{k=1}^{N} \cos \frac{(k-1)j\pi}{N} \cos \frac{kj\pi}{N} = \frac{N}{2} \cos \frac{j\pi}{N} \quad \text{(A3)}$$

where j is any integer. Substituting Eqs. (21), (A2), and (A3) into Eq. (A1) yields the final expression for the modal mass in Eq. (23).

Acknowledgments

The research work in this paper was supported by the National Science Foundation under Grant BCS-8858549 and by the Ohsaki Research Institute of Shimizu Corporation. This support is gratefully acknowledged.

References

[1]Brillouin, L., *Wave Propagation in Periodic Structures,* Dover, New York, 1953, Chap. 1–4.

[2]Mead, D. J., "Wave Propagation and Natural Modes in Periodic Systems: I. Mono-Coupled Systems, II. Multi-Coupled Systems, With and Without Damping," *Journal of Sound and Vibration,* Vol. 40, 1975, pp. 1–39.

[3]Lin, Y. K., and Donaldson, B. K., "A Brief Survey of Transfer Matrix Techniques with Special Reference to the Analysis of Aircraft Panels," *Journal of Sound and Vibration,* Vol. 10, 1969, pp. 103–143.

[4]Yong, Y., and Lin, Y. K., "Propagation of Decaying Waves in Periodic and Piecewise Structures of Finite Length," *Journal of Sound and Vibration,* Vol. 129, 1989, pp. 99–118.

[5]Signorelli, J., and von Flotow, A. H., "Wave Propagation, Power Flow, and Resonance in a Truss Beam," *Journal of Sound and Vibration,* Vol. 126, 1988, pp. 127–144.

[6]Mead, D. J., "A New Method of Analyzing Wave Propagation in Periodic Structures; Applications to Periodic Timoshenko Beams and Stiffened Plates," *Journal of Sound and Vibration,* Vol. 104, 1986 pp. 9–27.

[7]Keane, A. J., and Price, W. G., "On the Vibrations of Mono-Coupled Periodic and Near-periodic Structures," *Journal of Sound and Vibration,* Vol. 128, 1989, pp. 423–450.

[8]Crandall, S. H., "Structured Response Patterns Due to Wide-Band Random Excitation," *Stochastic Problems in Dynamics,* edited by B. L. Clarkson, Pitman, London, 1977, pp. 366–389.

[9]Crandall, S. H., "Random Vibration of One- and Two-Dimensional Structures," *Developments in Statistics,* Vol. 2, 1979, pp. 1–82.

[10]Dowell, E. H., and Kubota, Y., "Asymptotic Modal Analysis and Statistical Energy Analysis of Dynamical Systems," *Journal of Applied Mechanics,* Vol. 52, 1985, pp. 949–957.

[11]Skudrzyk, E., *Simple and Complex Vibratory Systems,* Pennsylvania State Univ. Press, State College, PA, 1958, Chap. 11.

[12]Skudrzyk, E., "The Mean-Value Method of Predicting the Dynamic Response of Complex Vibrators," *Journal of the Acoustical Society of America,* Vol. 67, No. 4, 1980, pp. 1105–1135.

[13]Xu, K., "Dynamic Analysis and Control of Structures with Closely Spaced Natural Frequencies," Ph.D. Thesis, Dept. of Civil Engineering, Northwestern Univ., Evanston, IL, 1992.

[14]Lin, Y. K., *Probabilistic Theory of Structural Dynamics,* Krieger, Huntington, New York, 1967, Chap. 7.

[15]Faulker, M. G., and Hong, D. P., "Free Vibrations of a Mono-Coupled Periodic System," *Journal of Sound and Vibration,* Vol. 99, 1985, pp. 29–42.

[16]Challifour, J. L., *Generalized Functions and Fourier Analysis, an Introduction,* Benjamin, Reading, MA, 1972, Chap. 2.